Acta Cryst. (1959). **12**, 679

Structural Parameter Determination of Small Aromatic Systems in Non-Crystalline Solids

By W. Ruland

European Research Associates s.a., 95 rue Gatti de Gamond, Brussels 18, Belgium

(*Received* 23 *December* 1958 *and in revised form* 23 *February* 1959)

The diffuse X-ray scattering from three non-crystalline polymers containing small aromatic ring systems has been investigated using Diamond's (1958) least-squares method. The structural parameters obtained, 'amorphous content', aromatic size distribution, mean layer size and mean bond length, are on the whole in good agreement with the theoretical values. The effect of deviations from an ideal aromatic system on the structural parameters is discussed.

Introduction

The determination of structural parameters in non-crystalline substances is very important in coal research. Diamond (1958) has recently described a method which contributes to the solution of this problem. The present work is concerned with the applicability of this method to the analysis of the diffuse scattering of X-rays from non-crystalline substances containing small aromatic systems. Three polymers of known composition, none of which had any crystalline content, have been used: poly(α-allylnaphthalene) (PAN), poly(9-allylfluorene) (PAF) and a naphthylene (1,5- and 1,8-) urea polymer (PNU).

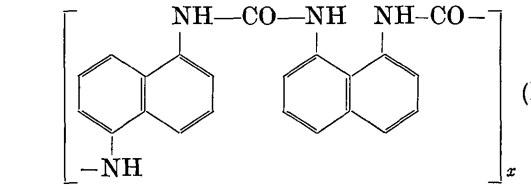

(PNU)

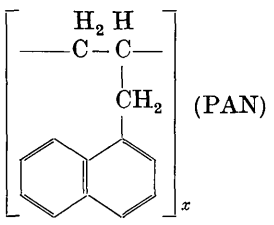

(PAN)

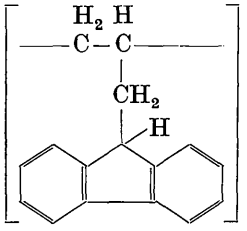

(PAF)

Experimental

Measurements were made on a Norelco counter diffractometer using a Philips–Eindhoven xenon-filled proportional counter (dead time *ca.* 2 μsec.) as detector. The counting rate was usually between 400 and 800 counts per second which is well within the linear region of the counter.

Ross's (1928) difference-filter method was used to obtain effectively monochromatic Cu $K\alpha$ radiation. The filters were prepared by mixing the appropriate oxides (NiO or Co_2O_3) with polythene powder and pressing into discs. By choosing the correct oxide contents, a pair of filters was prepared whose absorption curves were practically identical outside the region between the Ni and Co K absorption edges and had the optimum difference within this region. In this way the effective intensity was much greater than would normally be obtained by the use of crystal-monochromatized radiation. The white radiation between the two absorption edges had a negligible effect on the scattering curves obtained.

The filters were placed between specimen and counter so that only that part of the scattered radiation which lies between the two absorption edges was measured. In the angular range used this includes Compton scattering but excludes all fluorescent K radiation. This is a very important consideration as it is extremely difficult to remove the last traces of iron from coal samples and the fluorescent radiation produced forms a considerable proportion of the total X-ray scattering. In order to assess the importance of this effect an Al filter was made having the same absorption as the Ni and Co filters below their absorption edges. The difference between the transmissions of the Co and Al filters gives the long-

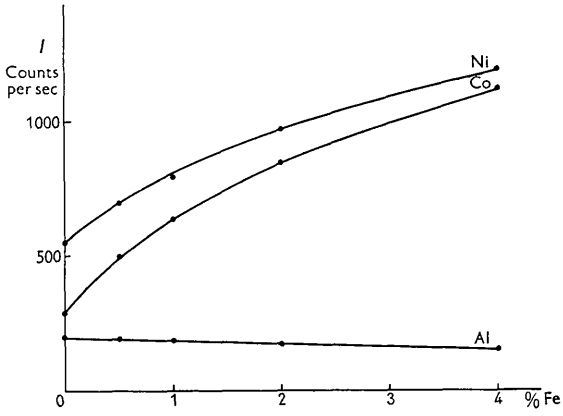

Fig. 1. The effect of iron on the scattered radiation intensity.

wavelength portion of the scattering. Measurements were made at $\theta = 30{\cdot}5°$ with spectroscopic carbon (National Carbon Company type SP2) containing varying amounts of added iron oxide (Fig. 1). The difference between the transmissions of the two filters due to Fe K radiation increases rapidly with increasing iron content and already at 0·5% Fe is of the same order as the sum of the measured coherent and Compton scattering from the carbon. Thus unless the secondary beam is monochromatized precise intensity measurements are impossible.

Because of the low absorption it is necessary to take into account X-ray scattering from the interior as well as from the surface of the specimen. Its thickness (d) was so chosen that at the maximum θ used (*ca.* 50°), $2\mu d/\sin\theta > 5$ where μ is the absorption coefficient. The loss of scattered intensity due to low absorption was thus less than 0·7%. Following Milberg (1958), a larger collimator aperture was used than would normally be required for the size of counter aperture chosen in order to irradiate all the specimen within the field of view of the counter. Keating & Warren (1952) have calculated corrections to eliminate the smearing of the scattering curve due to scattering from the whole thickness of the specimen. In the present work this correction did not change the shapes of the scattering curves but displaced them slightly towards lower angles. This displacement was later taken into account in the calculation of mean bond lengths. The air scattering was of the order of 0·2% of the total scattering and was neglected.

Each intensity curve was recorded eight times and measured at equal intervals of $s = 2\sin\theta/\lambda$. The mean of the eight measurements at each point had a statistical error of less than 1%.

Results

The 31 intensity values at $0{\cdot}66 \le s \le 0{\cdot}96$ are, after correction for polarization, considered as the elements of the vector **I**. (Diamond's notation is used throughout). The vector $\boldsymbol{\lambda}$ obtained by premultiplying **I** by the matrix $\mathbf{H}_5$ will be designated $\boldsymbol{\lambda}_{\text{exp.}}$ when it is derived from experimental intensity data. Diamond suggested that in a size-distribution calculation it would be necessary to make allowance for errors introduced into the **B** matrix by the use of Compton & Allison's (1935) values for the incoherent scattering factor instead of the new values of Keating & Vineyard (1956) and also for the effect of foreign atoms.

A two-stage correction has been developed to achieve this. (Diamond has independently devised a somewhat similar correction.) Equation (1) corrects $\boldsymbol{\lambda}_{\text{exp.}}$ for the errors in the values of the Compton effect and eliminates the need for recalculating the $\mathbf{H}_5$ matrix. Equation (2) will eliminate an additive contribution to the scattering curve and for this reason can only be used to remove foreign atom effects from $\boldsymbol{\lambda}$ when these atoms are in the 'amorphous' part of the structure and scatter incoherently with respect to the aromatic system. The hydrogen contribution can always be so removed since its coherent scattering factor is negligible in the s range used.

$$\boldsymbol{\lambda} = \frac{\boldsymbol{\lambda}_{\text{exp.}}}{\Sigma\lambda_{\text{exp.}}}(1-\Sigma\lambda_{\Delta}) + \boldsymbol{\lambda}_{\Delta} \qquad (1)$$

where $\boldsymbol{\lambda}_{\Delta} = \mathbf{H}_5\mathbf{I}_{\Delta}$ and $\mathbf{I}_{\Delta}$ is the difference between Compton & Allison's, and Keating & Vineyard's values for the incoherent scattering of carbon.

$$\boldsymbol{\lambda}_j = \boldsymbol{\lambda}\Sigma\frac{N_i}{N_j}\Sigma\lambda_i - \sum_{i\neq j}\frac{N_i}{N_j}\boldsymbol{\lambda}_i \qquad (2)$$

where

$$\boldsymbol{\lambda}_i = \mathbf{H}_5\mathbf{I}_i + \frac{\Sigma H_5 I_i}{(1-\Sigma\lambda_{\Delta})}\boldsymbol{\lambda}_{\Delta}\,.$$

I_i is the normalized scattering intensity of atom type i and N_i is the number of atoms of type i.

Equation (2) can be used to remove the effect of foreign atoms in the 'amorphous' part of the structure so that $\boldsymbol{\lambda}_j$ represents the scattering from the aromatic part of the structure and the amorphous carbon. In Table 1 are given values of $\boldsymbol{\lambda}_{\Delta}$, $\boldsymbol{\lambda}_{\text{H}}$, $\boldsymbol{\lambda}_{\text{N}}$ and $\boldsymbol{\lambda}_{\text{O}}$

Table 1. $\boldsymbol{\lambda}$ *vectors*

λ	$\boldsymbol{\lambda}_{\Delta}$	$\boldsymbol{\lambda}_{\text{H}}$	$\boldsymbol{\lambda}_{\text{N}}$	$\boldsymbol{\lambda}_{\text{O}}$
A	0·10558	0·07333	1·75339	2·78031
5·8	−0·08893	0·08730	−0·85422	−1·86522
8·4	0·00570	−0·01080	0·11351	0·23567
10	0·03747	−0·03918	0·41975	0·89327
15	0·00948	−0·00551	0·03902	0·09843
20	−0·01863	0·02305	−0·25613	−0·53617
30	0·00323	−0·00691	0·09194	0·18212
$\Sigma\lambda_i$	0·05390	0·12128	1·30726	1·78841

calculated using the coherent scattering factors of Berghuis *et al.* (1955) and the incoherent scattering factors of Keating & Vineyard for carbon in the valence state and of Milberg & Brailsford (1958) for oxygen in the ground state. The Compton scattering of nitrogen was taken as the mean of Milberg & Brailsford's values for carbon and oxygen. The Breit–Dirac recoil factor was not applied as its effect is less than the difference between the ground-state and valence-state values for the Compton scattering. The scattering functions were subtabulated at intervals of $s = 0{\cdot}01$ by the method of bridging differences (Hartree, 1952).

Fig. 2 shows the histograms obtained from the scattering curves of the three polymers; (*a*) are uncorrected values and (*b*) are corrected using equations (1) and (2). In the case of PNU the nitrogen has been assumed to scatter coherently with the aromatic system.

Theoretical scattering curves of the aromatic parts of the three polymers were calculated using Debye's equation

$$I = \frac{1}{N}\left[\sum_i\sum_j f_i f_j \frac{\sin 2\pi r_{ij}s}{2\pi r_{ij}s} + I_{\text{incoherent}}\right]. \qquad (3)$$

Table 2. *Comparison of experimental and theoretical values*

	PAN				PAF				PNU		
	exp.	corr.	theor.	theor. +temp.	exp.	corr.	theor.	theor. +temp.	exp.	corr.	theor.
A %	18·6	24·6	20·4	23·7	29·8	36·4	37·3	36·6	23·7	15·6	14·4
$\bar{L}$ (Å)	5·7	5·9	5·6	5·6	6·1	6·3	6·5	6·8	7·0	7·0	6·1
$\bar{N}$	11	11	10	10	12	13	13	15	16	16	12

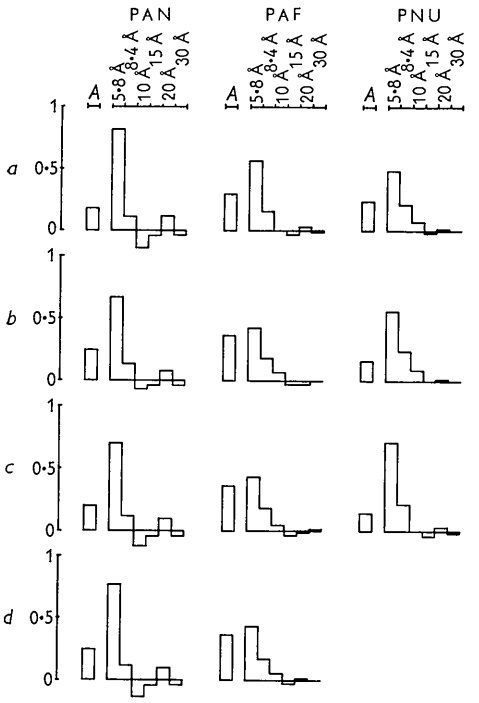

Fig. 2. Histograms of the three polymers. (*a*) Uncorrected. (*b*) Corrected. (*c*) Theoretical. (*d*) Theoretical with temperature factor.

Burns & Iball's (1955) data were used for the dimensions of the fluorene molecule; the naphthalene C–C bond and the $C_{arom.}$–N bond in PNU were both taken as 1·405 Å and the $C_{arom.}$–$C_{aliph.}$ bond in PAN was taken as 1·540 Å. Histograms obtained from these theoretical scattering curves are shown in Fig. 2(*c*). The histograms of Fig. 2(*d*) are based on theoretical scattering curves to which a temperature factor corresponding to an r.m.s. vibration of 0·06 Å has been applied. Table 2 gives the values for the 'amorphous content' A, the mean layer diameter $\bar{L}$, and the average number of atoms per layer $\bar{N}$, obtained from the different histograms.

The mean bond lengths $\bar{a}$ were determined both by the method given in Diamond's paper and by the following graphical method. If the experimental scattering curve and the least-squares curve $\mathbf{B'\lambda}_{exp.}$ are plotted against $\log s$ they can be more or less superposed by relative displacement in the $\log s$ direction. The displacement $\Delta \log s$ of $I_{exp.}$ necessary is related to the mean bond length by

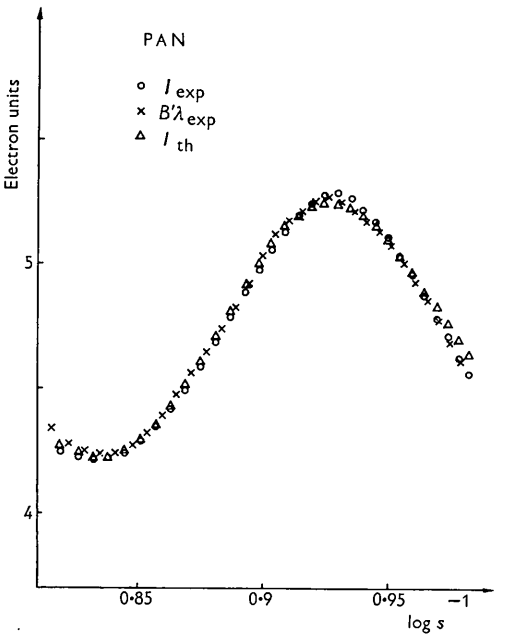

Fig. 3. Comparison of calculated and experimental scattering curves for PAN.

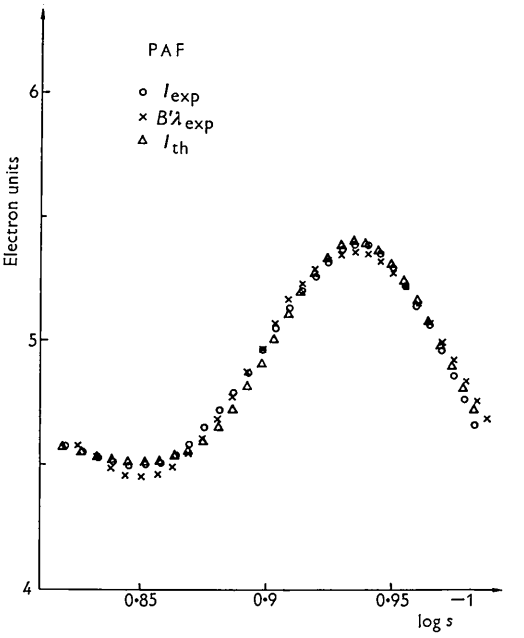

Fig. 4. Comparison of calculated and experimental scattering curves for PAF.

$$\bar{a} = 1{\cdot}405(1+2{\cdot}3\Delta \log s) \text{ Å} . \quad (4)$$

This method assumes that, to a first approximation, the scattering curve of an aromatic system is a function of $\bar{a}s$ and that $2{\cdot}3\Delta \log s \ll 1$. It has the advantage over the analytical method that the goodness of fit of the two curves is an indication of the validity of the least-squares method. Both methods gave identical results which are shown in Table 3.

Table 3. *Apparent mean bond lengths*

	$\bar{a}$ (Å)
PAN	1·413
PAF	1·392
PNU	1·402

The experimental scattering curve, the least-squares curve $\mathbf{B}'\lambda$ and the theoretical curve, all

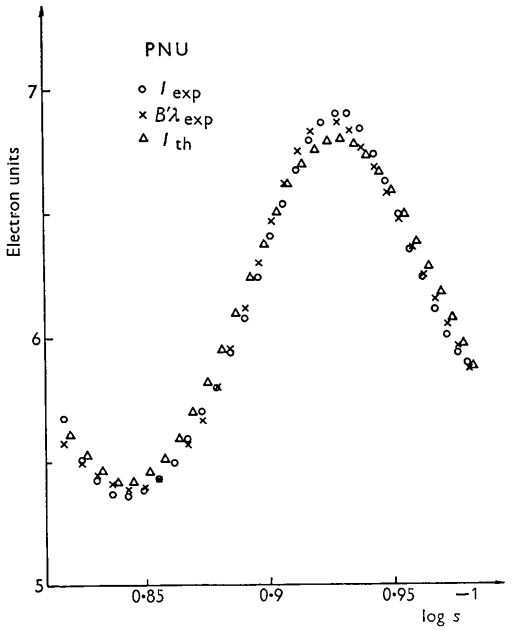

Fig. 5. Comparison of calculated and experimental scattering curves for PNU.

normalized to the scattering for one atom, are shown for the three substances in Figs. 3, 4 and 5.

Discussion

A comparison of the experimental curves with those calculated assuming additivity of the scattering contributions shows that in the region investigated ($0{\cdot}66 \leq s \leq 0{\cdot}96$) there is no discernible effect due to intermolecular ordering. In the case of PAN and PAF there is good agreement between experimental and calculated values. The application of equations (1) and (2) affects mainly the value of the 'amorphous content'. In view of this good agreement, the high experimental value of the layer size in PNU is unlikely to be due to experimental error. It seems probable that the layer size is effectively increased by the tendency of the –NH–CO– group to be ordered with respect to the naphthylene residue. This hypothesis is supported by the fact that the first intermolecular scattering maximum lies at a higher angle than that of PAN or PAF. Assuming parallel stacking, this maximum would correspond to an interlayer spacing of 3·7 Å which is a normal value for aromatic layers.

The results obtained with PAF show that for a small system the values of the layer size are good in spite of the irregularities due to the five-membered ring. However, the mean bond-length calculation is meaningless when the structure contains such irregularities. In the case of the small hexagonal networks which have been studied, the calculated mean bond lengths agree well with the arithmetic means of the lengths of the bonds in the aromatic system together with those between the rings and their nearest neighbours.

The introduction of disorder into the hexagonal network will change the value of the 'amorphous carbon content'. Thus, the effect of thermal motion can be seen from a comparison of the theoretical values with and without allowance for the temperature factor (Table 2). The effect of distortions such as introduced by five-membered rings and side groups containing foreign atoms or having bond lengths different from those in the hexagonal system is shown by the theoretical calculations in which these deviations have been taken into account. In all three cases the 'amorphous carbon content' is found to be greater than that which would be expected from the structural formula (PAN: 2/13 = 15·4%, PAF: 3/16 = 18·8%, PNU: 1/13 = 7·7%).

The higher value of Ath for PNU does not conflict with the hypothesis that the increase in $\bar{L}$ is due to a partial ordering of the side groups with respect to the aromatic layers since A and $\bar{L}$ do not depend in the same way on the disorder. Thus, in the case of PAF the value of $\bar{L}$ is not affected by the five-membered ring while the value of Ath is increased.

This work is part of a project sponsored by the Union Carbide Corporation, New York, and I take this opportunity to express my appreciation of this support. I thank Dr R. H. Gillette for his continued encouragement and interest in this work. I have had many stimulating and helpful discussions with Dr P. B. Hirsch and Dr H. Tompa to both of whom I am grateful. I am also indebted to the staff of the IBM installation in this laboratory for carrying out the calculations.

References

Berghuis, J., Haanappel, IJ. M., Potters, M., Loopstra, B. O., MacGillavry, C. H. & Veenendaal, A. L. (1955). *Acta Cryst.* 8, 478.

BURNS, D. M. & IBALL, J. (1955). *Proc. Roy. Soc.* A, **227**, 200.
COMPTON, A. H. & ALLISON, S. K. (1935). *X-rays in Theory and Experiment.* New York: Van Nostrand.
DIAMOND, R. (1958). *Acta Cryst.* **11**, 129.
HARTREE, D. R. (1952). *Numerical Analysis.* Oxford: Clarendon Press.
KEATING, D. T. & VINEYARD, G. H. (1956). *Acta Cryst.* **9**, 895.
KEATING, D. T. & WARREN, B. E. (1952). *Rev. Sci. Instrum.* **23**, 519.
MILBERG, M. E. (1958). *J. Appl. Phys.* **29**, 64.
MILBERG, M. E. & BRAILSFORD, A. D. (1958). *Acta Cryst.* **11**, 672.
ROSS, P. A. (1928). *J. Opt. Soc. Amer.* **16**, 433.

Acta Cryst. (1959). **12**, 683

The Effect of Segregation on the Diffraction from a Face-Centred Cubic Alloy with Deformation Faults

BY B. T. M. WILLIS

Atomic Energy Research Establishment, Harwell, Berks, England

(*Received* 9 *October* 1958 *and in revised form* 16 *March* 1959)

The Paterson theory of X-ray scattering from a face-centred cubic structure with deformation faults is extended to include the case of a f.c.c. alloy, in which segregation of the alloy components takes place at the faults. The principal effect of segregation is to make the reflexions asymmetrical. It is possible that this asymmetry could be detected in the powder lines of certain cold-worked alloys.

1. Introduction

Suzuki (1952) has suggested a hardening mechanism for face-centred cubic alloys, involving a segregation of solute atoms at deformation stacking faults. Segregation can occur because the crystal structure is close-packed hexagonal in a layer two atoms thick at the stacking fault; the concentration of solute atoms at the fault will therefore differ from the average, when the faulted region is in thermodynamic equilibrium with the surrounding cubic phase. Using this idea Suzuki has explained certain mechanical properties of alloys (see also Cottrell, 1954), but so far no direct evidence for segregation has been obtained. It is possible that such evidence could be provided by X-ray diffraction.

The purpose of this paper is to calculate the nature of the X-ray scattering from a deformation-faulted f.c.c. alloy, in which the alloy composition at the faults differs from that in the cubic matrix. We thus require to extend the treatment of Paterson (1952), dealing with the diffraction from a homogeneous, faulted f.c.c. crystal, to include the case of segregation.

2. Intensity distribution in reciprocal space

(*a*) *General formula*

Fig. 1(*a*) illustrates the stacking sequence of the close-packed (111) layers, with the faulted positions denoted by F, and f_1, f_2 representing the scattering powers averaged over the atoms in the two kinds of layer. When several faults occur in succession, the c.p.h. structure is developed only at the boundaries of the set, so that segregation takes place only at the kinks in the 'stacking line'.

The theory developed in this section assumes that there is no change of layer spacing accompanying segregation. The extension of the theory to include both change of scattering power and of spacing is considered in the Appendix, but it is shown there that the simpler theory of this section is adequate for most cases.

We make the usual assumption that faulting is restricted to one set of (111) planes only: the limitations imposed by this assumption have been considered by Willis (1958).

At first, the treatment follows very closely that given by Warren & Warekois (1955) for the problem of deformation-faulting without segregation.

It is convenient to choose hexagonal axes $\mathbf{A}_1$, $\mathbf{A}_2$, $\mathbf{A}_3$, with $\mathbf{A}_1$, $\mathbf{A}_2$ in the (111) plane and $\mathbf{A}_3$ normal to this plane. If $\mathbf{a}_1$, $\mathbf{a}_2$, $\mathbf{a}_3$ are the cubic axes of the unfaulted structure, then

$$\left.\begin{aligned} \mathbf{A}_1 &= -\mathbf{a}_1/2+\mathbf{a}_2/2 \\ \mathbf{A}_2 &= -\mathbf{a}_2/2+\mathbf{a}_3/2 \\ \mathbf{A}_3 &= \mathbf{a}_1/3+\mathbf{a}_2/3+\mathbf{a}_3/3\,. \end{aligned}\right\} \qquad (1)$$

Similar equations relate the corresponding hexagonal H_1, H_2, H_3 and cubic hkl indices:

$$\left.\begin{aligned} H_1 &= -h/2+k/2 \\ H_2 &= -k/2+l/2 \\ H_3 &= h/3+k/3+l/3\,. \end{aligned}\right\} \qquad (1a)$$